Supplementary for: Large difference in aerosol radiative effects from BVOC-SOA treatment in three ESMs

Moa K. Sporre[1,2], Sara M. Blichner[1], Roland Schrödner[3], Inger H. H. Karset[1], Terje K. Berntsen[1,4], Twan van Noije[5], Tommy Bergman[5,6], Declan O'Donnell[7], and Risto Makkonen[7,8]

[1]Department of Geosciences, University of Oslo, Postboks 1022 Blindern, 0315 Oslo, Norway
[2]Now at: Department of Physics, Lund University, Box 118, 22100 Lund, Sweden
[2]Institute for Tropospheric Research, Permoserstr. 15, 04318 Leipzig, Germany
[4]CICERO Center for International Climate Research, Postboks 1129 Blindern, 0318 Oslo, Norway
[5]Royal Netherlands Meteorological Institute (KNMI), PO Box 201, 3730 AE De Bilt, the Netherlands
[6]Now at: Climate System Research, Finnish Meteorological Institute, P.O. Box 503, FI-00101, Helsinki, Finland
[7]Climate System Research, Finnish Meteorological Institute, P.O. Box 503, FI-00101, Helsinki, Finland
[8]Institute for Atmospheric and Earth System Research / Physics, Faculty of Science, University of Helsinki, P.O. Box 64, FI-00014, Finland

Correspondence: Moa Sporre (moa.sporre@nuclear.lu.se)

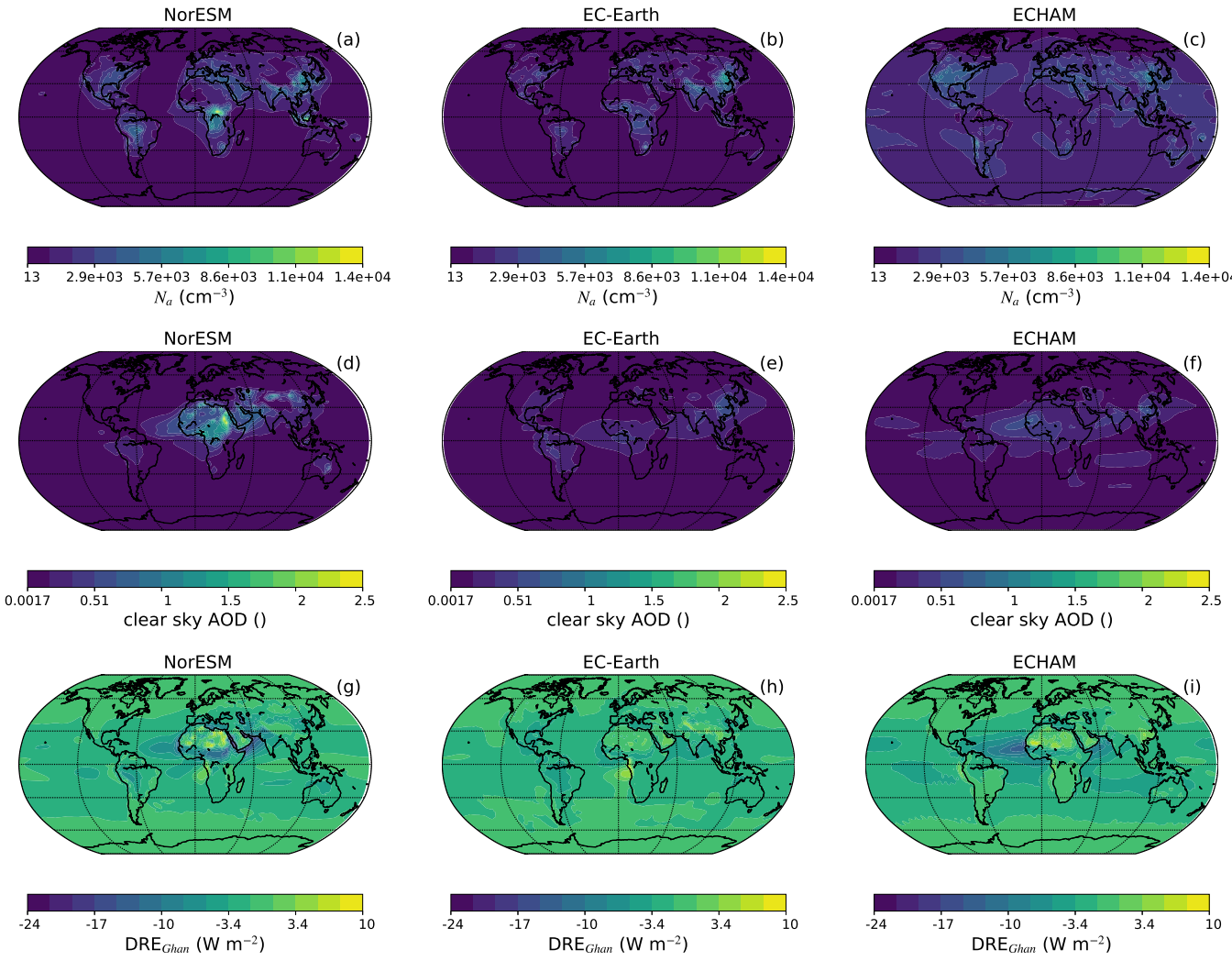

Figure S1. Maps of annually averaged total aerosol number concentration (a-c), clear sky aerosol optical depth (AOD) (d-f) and direct radiative effect (DRE$_{Ghan}$) (g-i) for NorESM, EC-Earth and ECHAM.

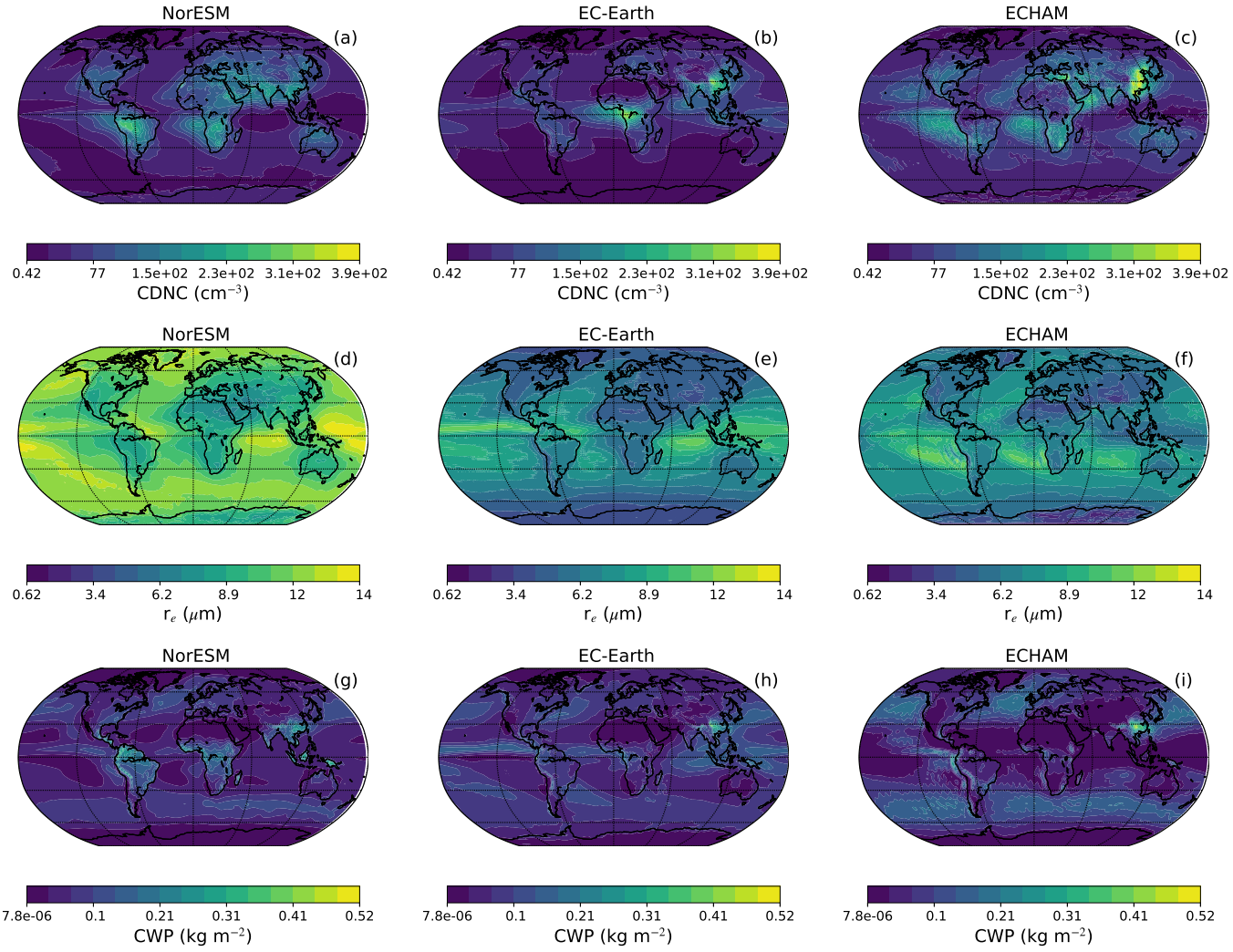

Figure S2. Maps of annually averaged in-cloud droplet number concentration (CDNC) at 860 hPa (a-c), in-cloud effective radius at 860 hPa (r_e) (d-f) and total gridbox cloud water path (CWP) (g-i) for NorESM, EC-Earth and ECHAM.

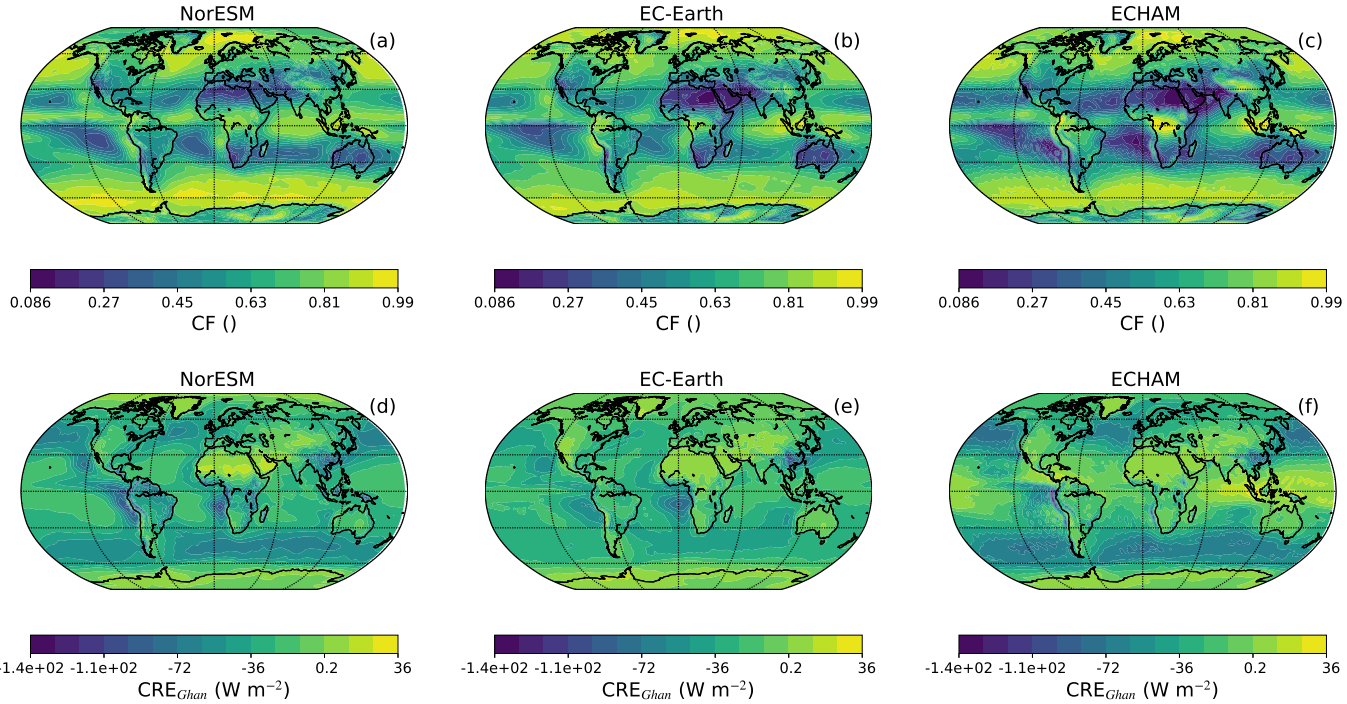

Figure S3. Maps of annually averaged cloud fraction (CF) (a-c) and cloud radiative effects (CRE$_{Ghan}$) (d-f) for NorESM, EC-Earth and ECHAM.

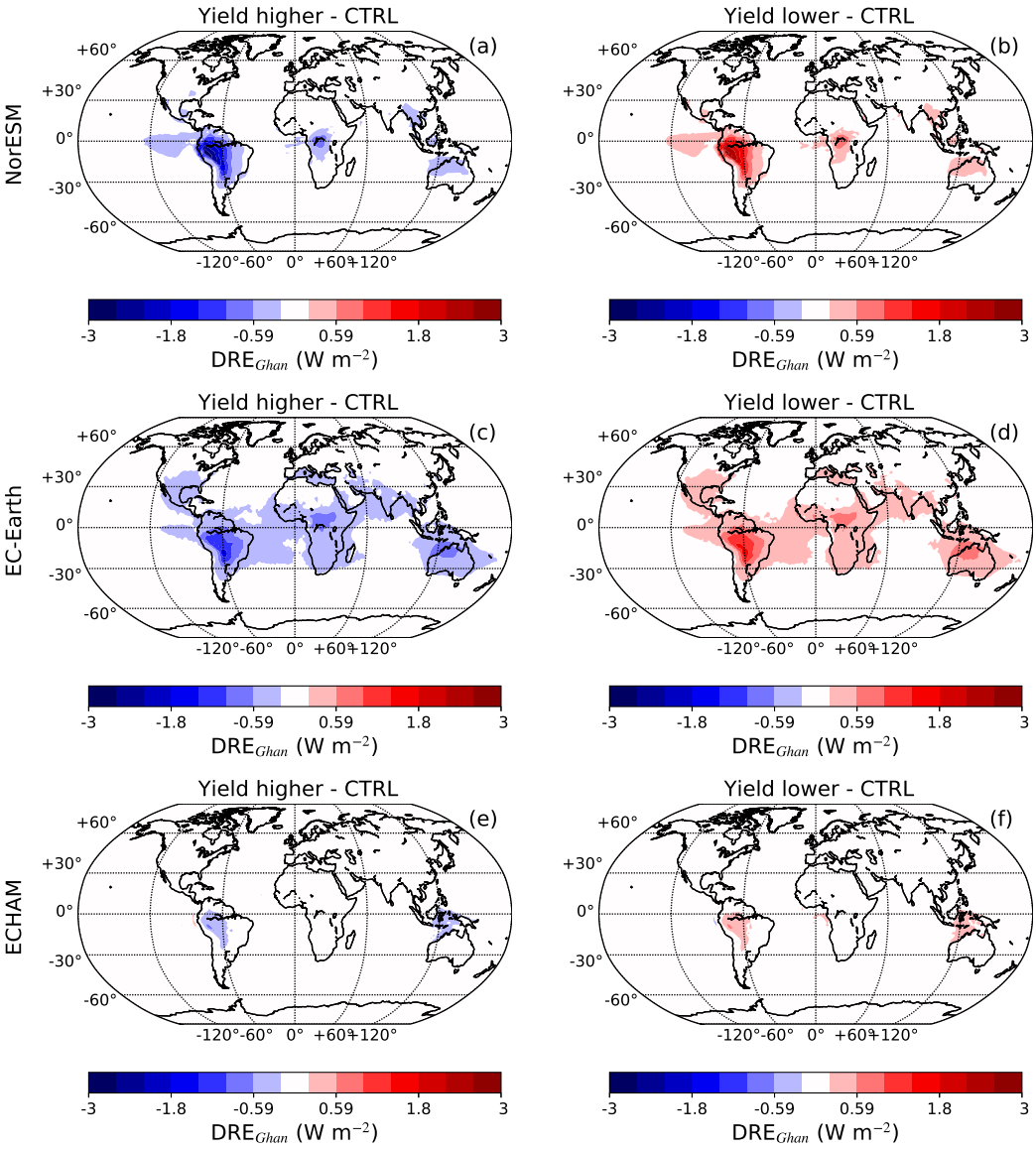

Figure S4. Maps of the difference in the average direct radiative effect (DRE$_{Ghan}$) between the Yield higher (a, c and e) and Yield lower (b, d and f) with respect to the CTRL simulation. This is shown for NorESM (a and b), EC-Earth (c and d) and ECHAM (e and f).

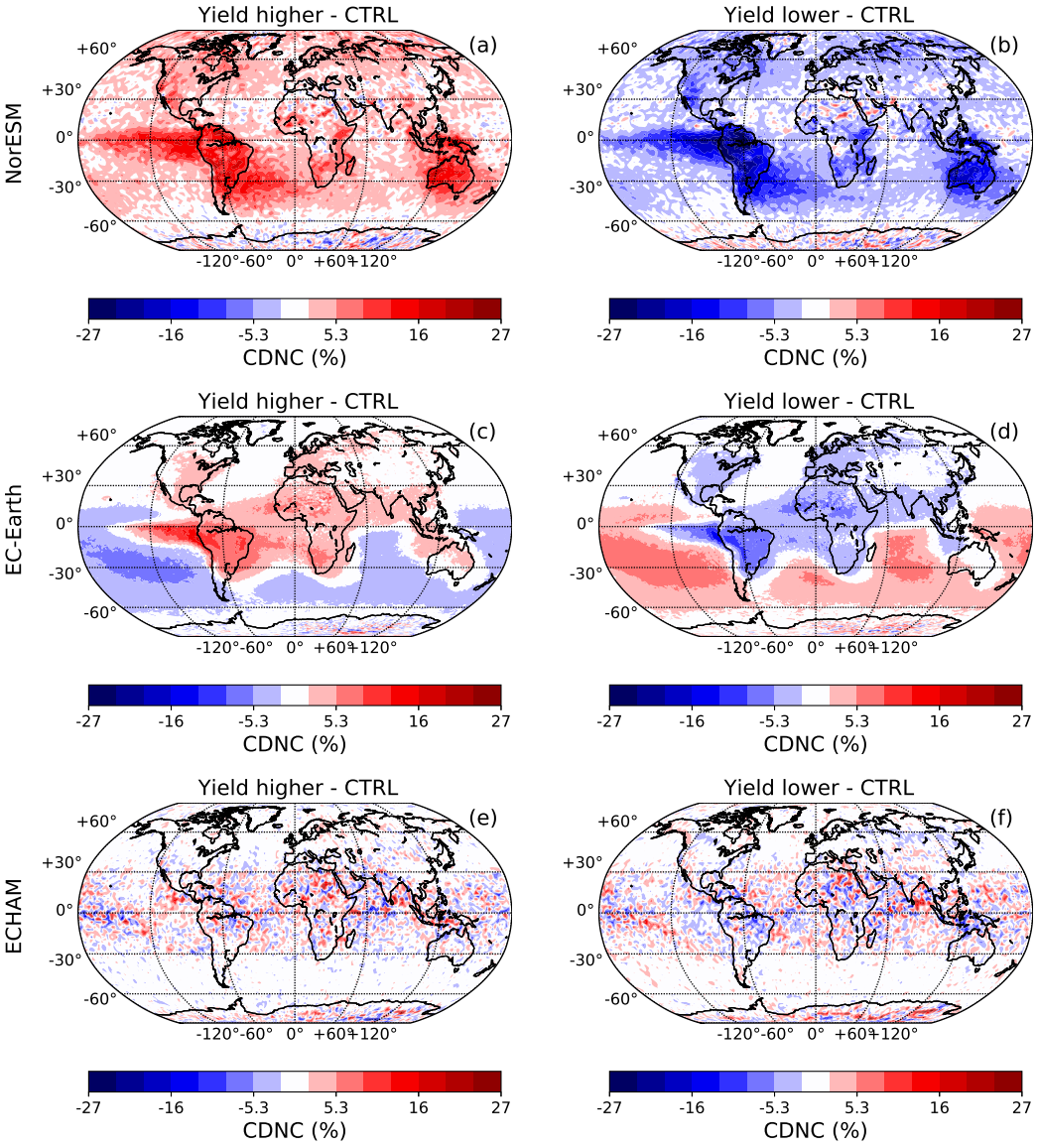

Figure S5. Maps of the difference in the average cloud cloud droplet number concentration (CDNC) between the Yield higher (a, c and e) and Yield lower (b, d and f) with respect to the CTRL simulation. This is shown for NorESM (a and b), EC-Earth (c and d) and ECHAM (e and f).

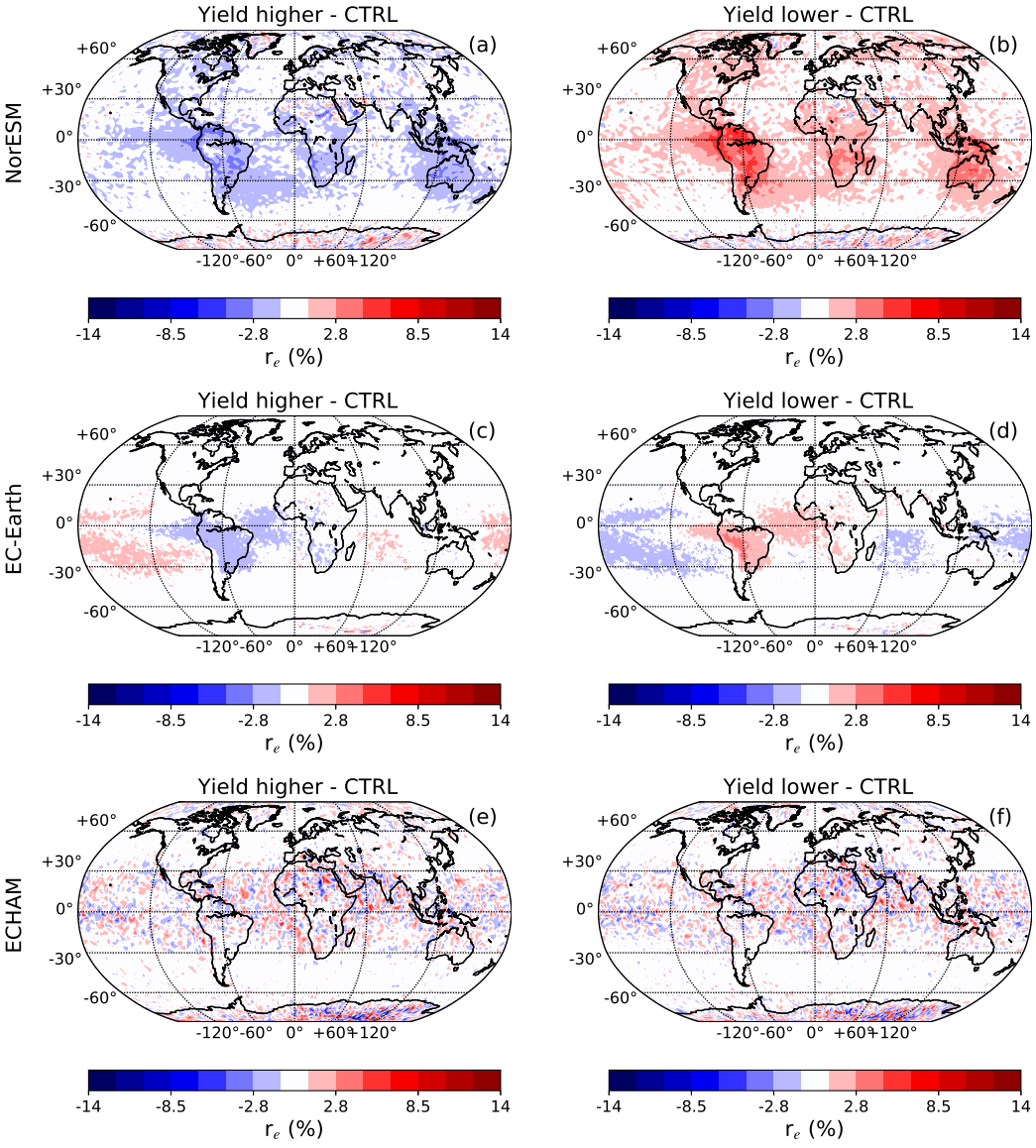

Figure S6. Maps of the difference in the average cloud cloud effective radius (r_e) between the Yield higher (a, c and e) and Yield lower (b, d and f) with respect to the CTRL simulation. This is shown for NorESM (a and b), EC-Earth (c and d) and ECHAM (e and f).

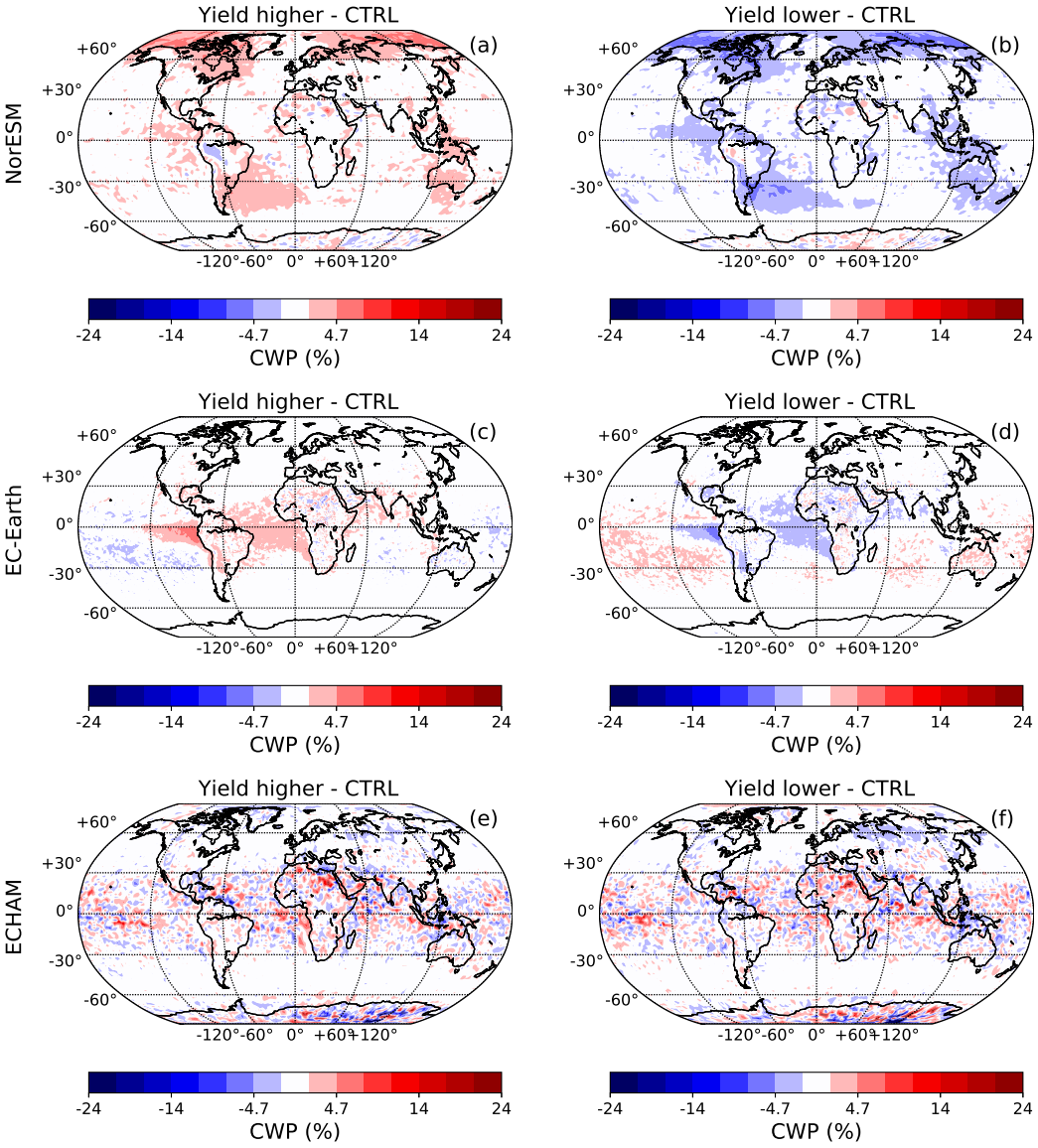

Figure S7. Maps of the difference in the average cloud water path (CWP) between the Yield higher (a, c and e) and Yield lower (b, d and f) with respect to the CTRL simulation. This is shown for NorESM (a and b), EC-Earth (c and d) and ECHAM (e and f).

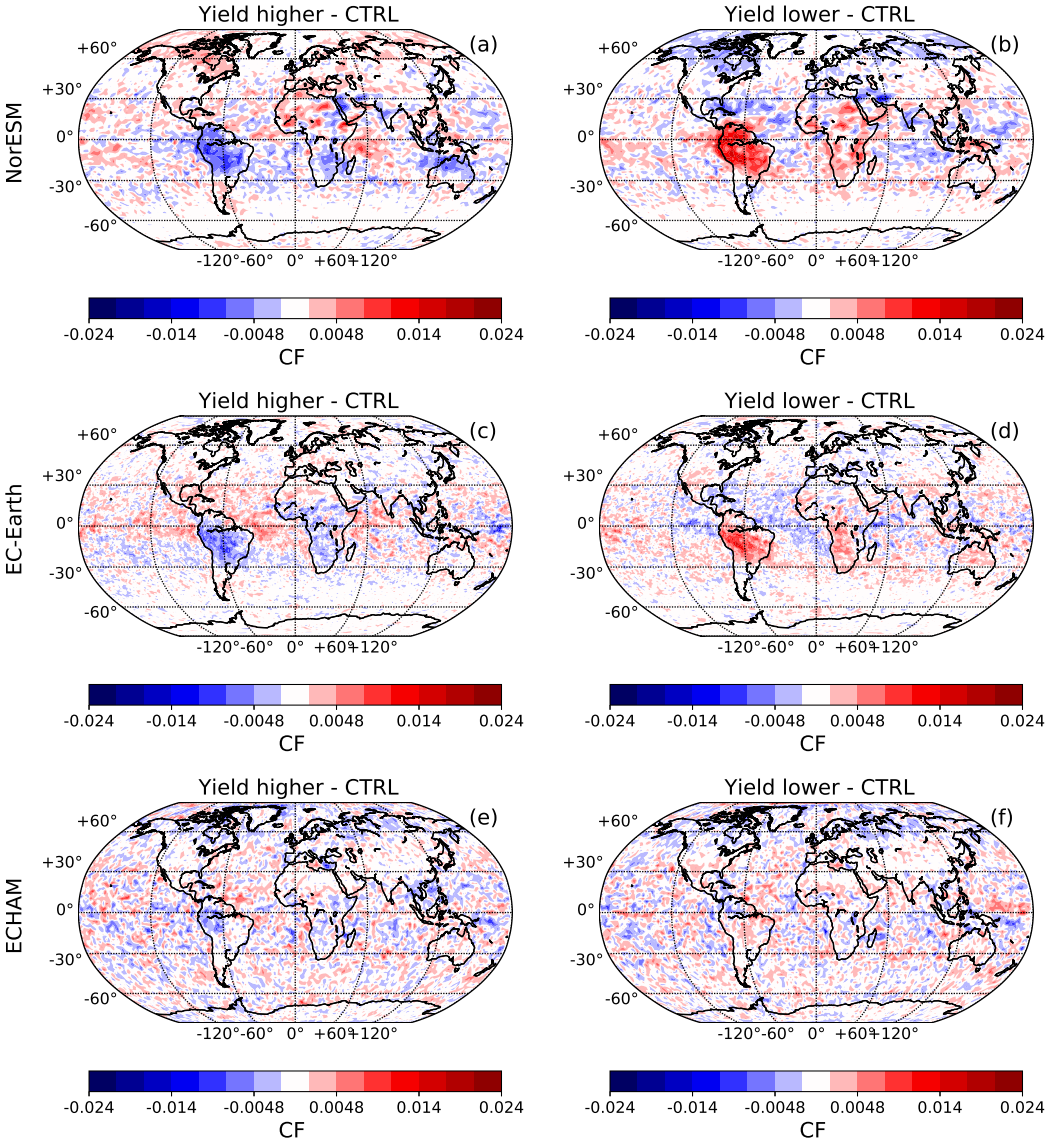

Figure S8. Maps of the difference in the average cloud fraction (CF) between the Yield higher (a, c and e) and Yield lower (b, d and f) with respect to the CTRL simulation. This is shown for NorESM (a and b), EC-Earth (c and d) and ECHAM (e and f).

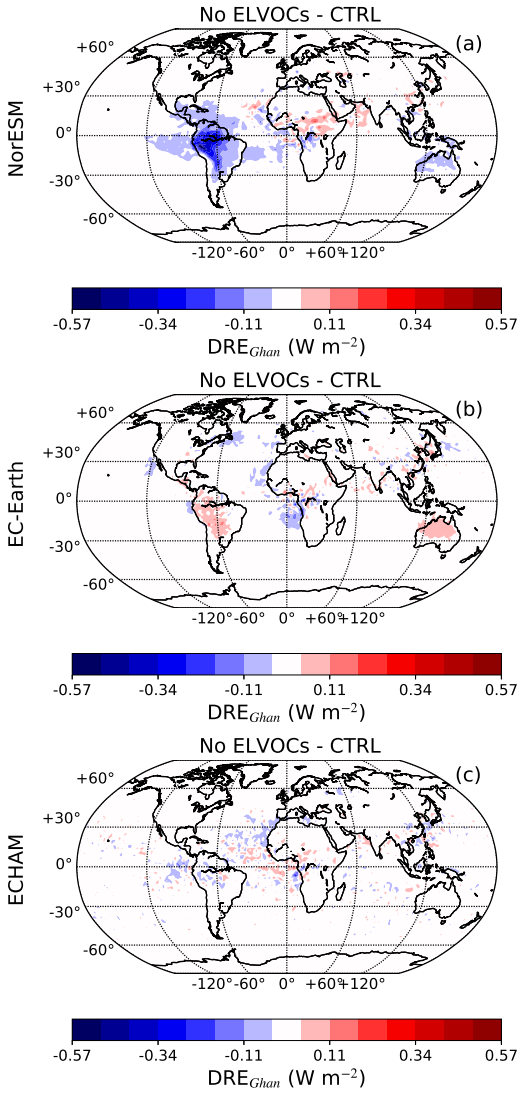

Figure S9. Maps of the difference in the average direct radiative effect (DRE$_{Ghan}$) between the No ELVOCs and the CTRL simulation. This is shown for NorESM (a), EC-Earth (b) and ECHAM (c).

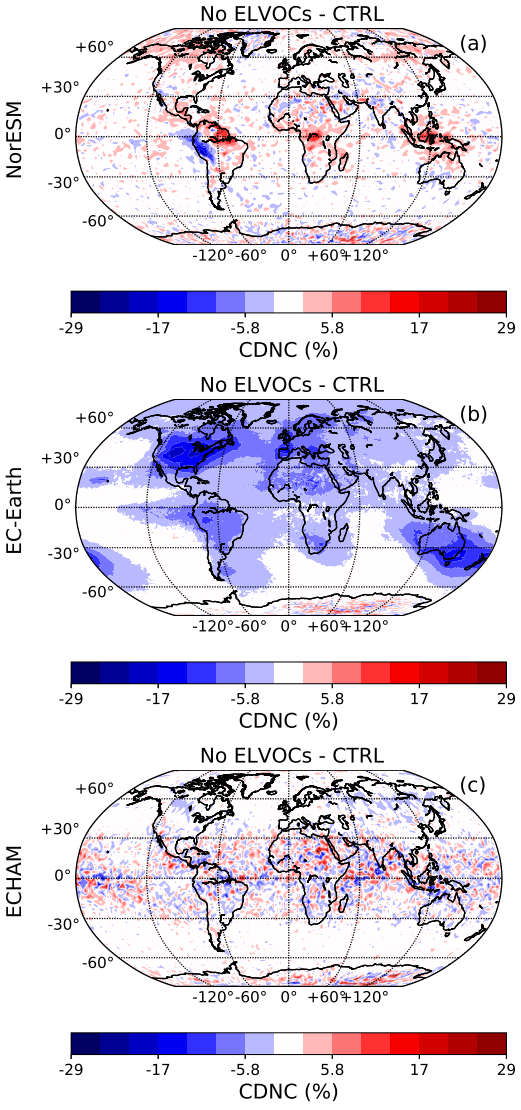

Figure S10. Maps of the difference in the average cloud cloud droplet number concentration (CDNC) between the No ELVOCs and the CTRL simulation. This is shown for NorESM (a), EC-Earth (b) and ECHAM (c).

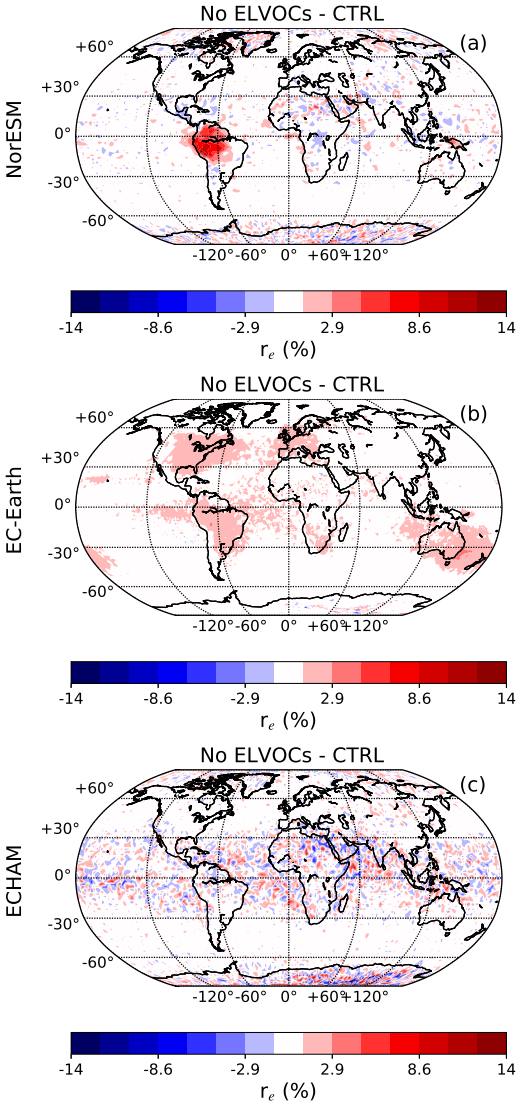

Figure S11. Maps of the difference in the average cloud cloud effective radius (r_e) between the No ELVOCs and the CTRL simulation. This is shown for NorESM (a), EC-Earth (b) and ECHAM (c).

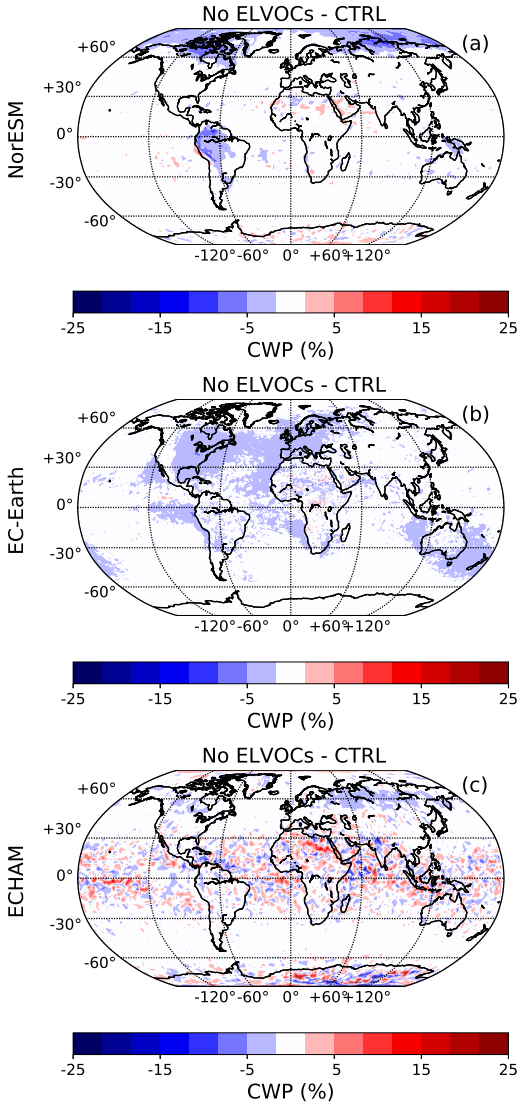

Figure S12. Maps of the difference in the average cloud water path (CWP) between the No ELVOCs and the CTRL simulation. This is shown for NorESM (a), EC-Earth (b) and ECHAM (c).

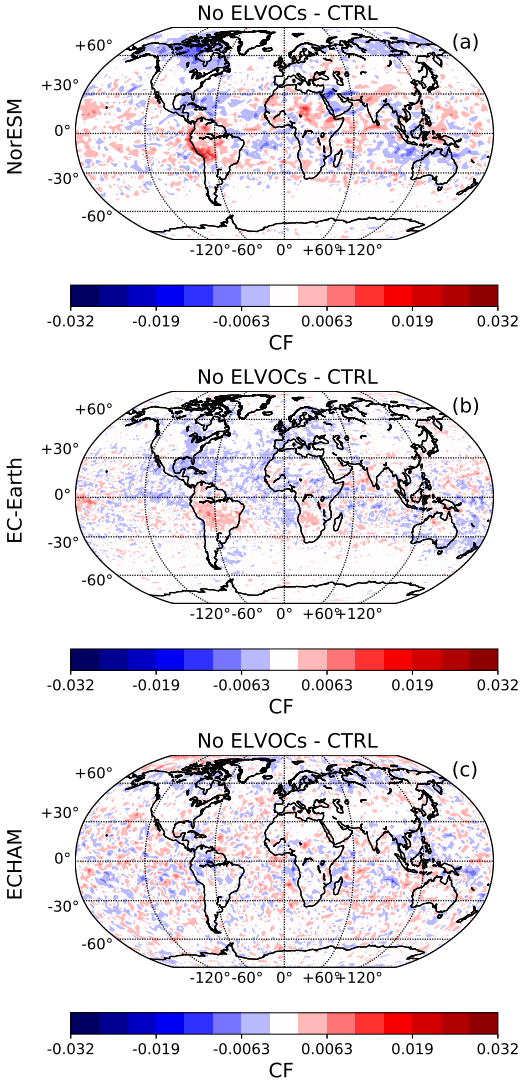

Figure S13. Maps of the difference in the average cloud fraction (CF) between the No ELVOCs and the CTRL simulation. This is shown for NorESM (a), EC-Earth (b) and ECHAM (c).

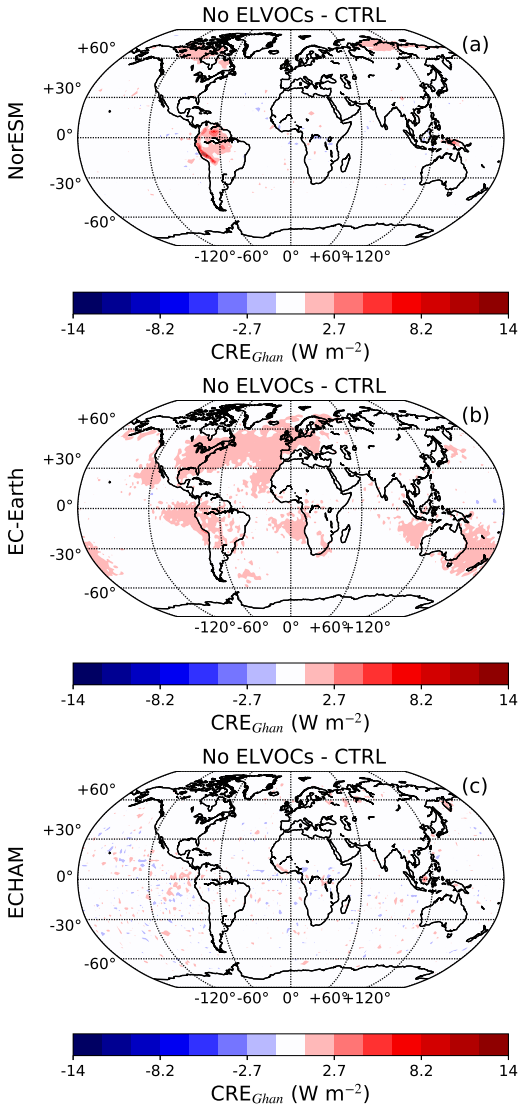

Figure S14. Maps of the difference in the average cloud radiative effect (CRE_{Ghan}) between the No ELVOCs and the CTRL simulation. This is shown for NorESM (a), EC-Earth (b) and ECHAM (c).

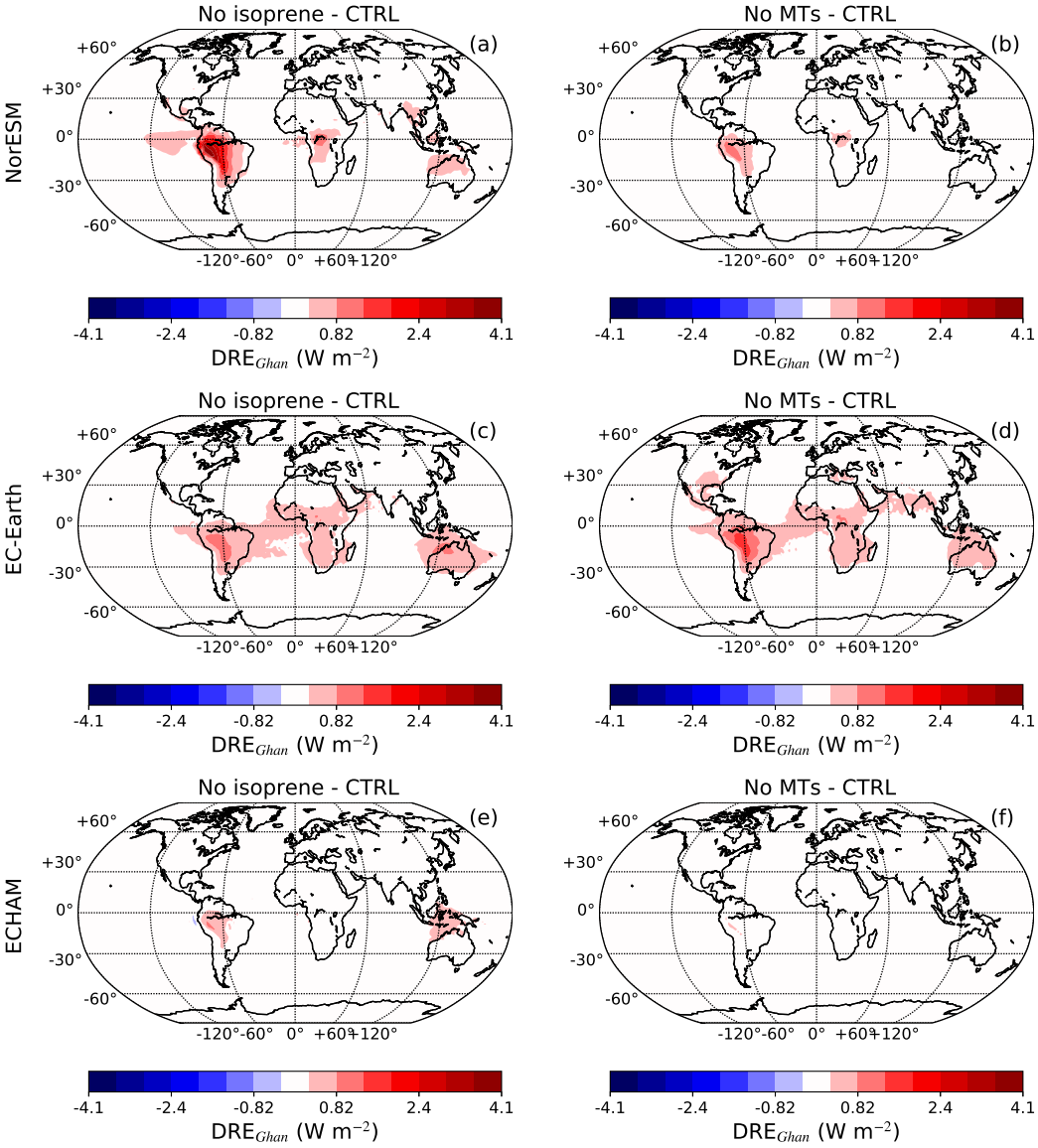

Figure S15. Maps of the difference in the average direct radiative effect (DRE$_{Ghan}$) between the No isoprene (a, c and e) and No MTs (b, d and f) with respect to the CTRL simulation. This is shown for NorESM (a and b), EC-Earth (c and d) and ECHAM (e and f).

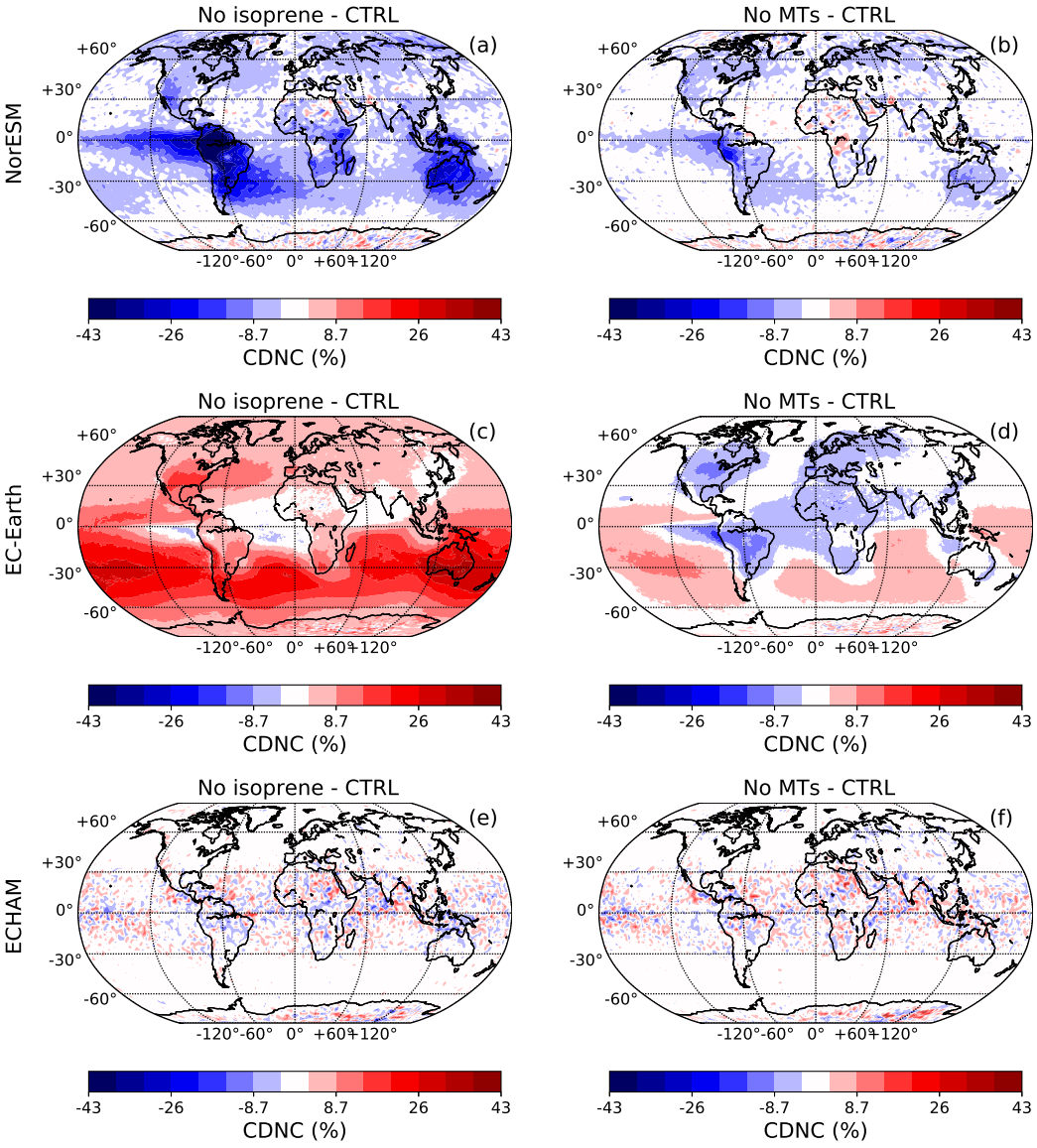

Figure S16. Maps of the difference in the average cloud cloud droplet number concentration (CDNC) between the No isoprene (a, c and e) and No MTs (b, d and f) with respect to the CTRL simulation. This is shown for NorESM (a and b), EC-Earth (c and d) and ECHAM (e and f).

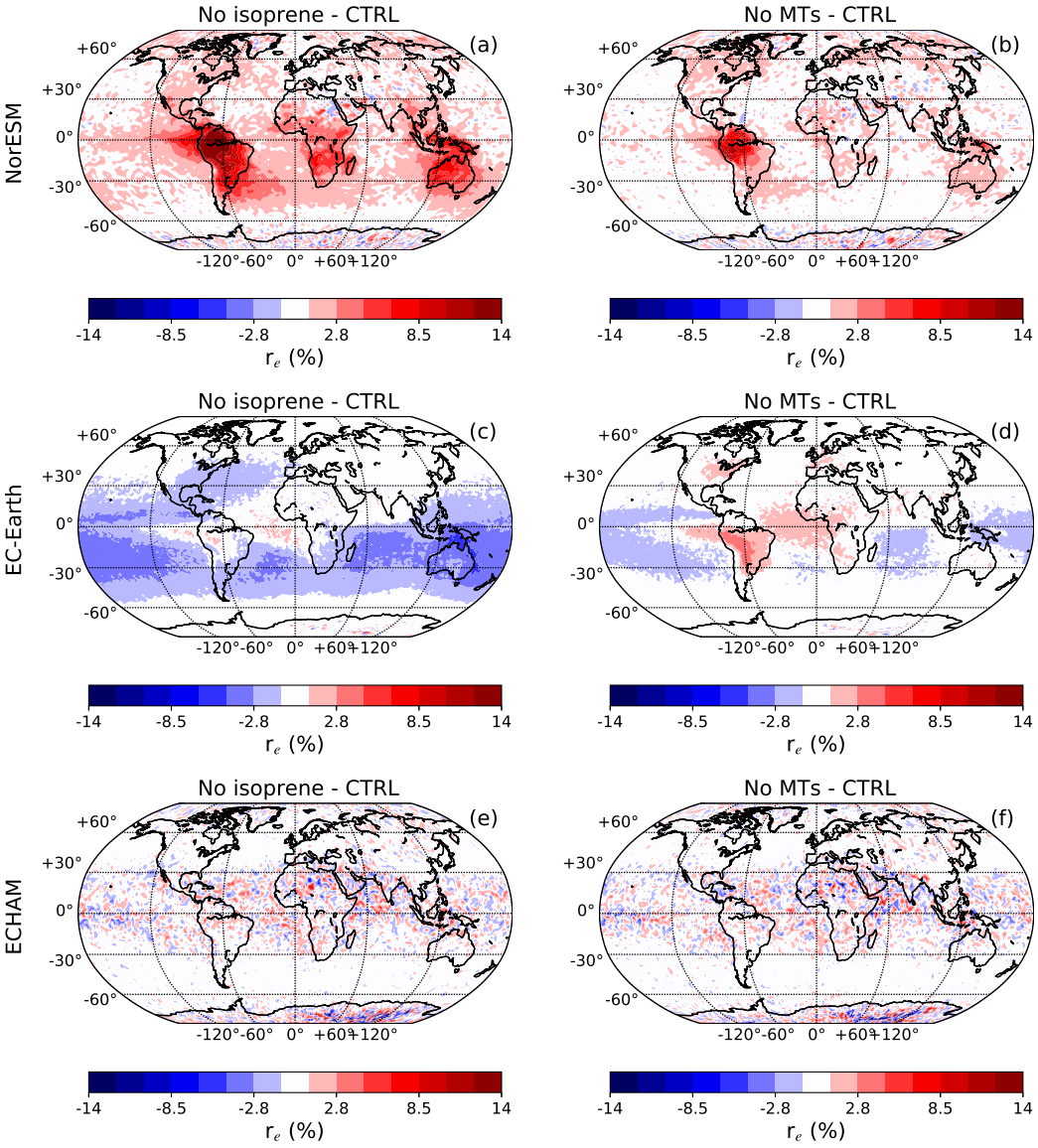

Figure S17. Maps of the difference in the average cloud cloud effective radius (r_e) between the No isoprene (a, c and e) and No MTs (b, d and f) with respect to the CTRL simulation. This is shown for NorESM (a and b), EC-Earth (c and d) and ECHAM (e and f).

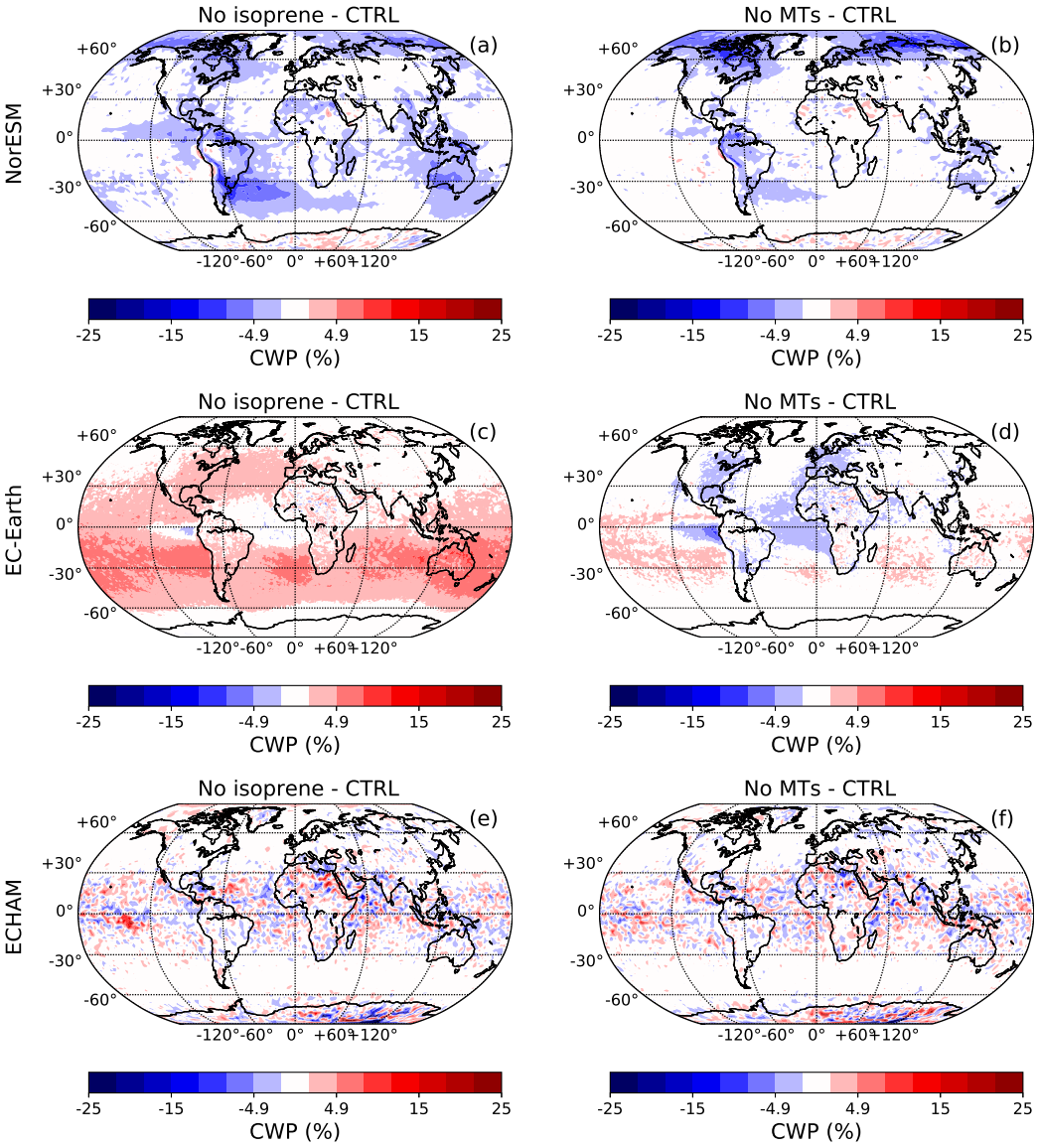

Figure S18. Maps of the difference in the average cloud water path (CWP) between the No isoprene (a, c and e) and No MTs (b, d and f) with respect to the CTRL simulation. This is shown for NorESM (a and b), EC-Earth (c and d) and ECHAM (e and f).

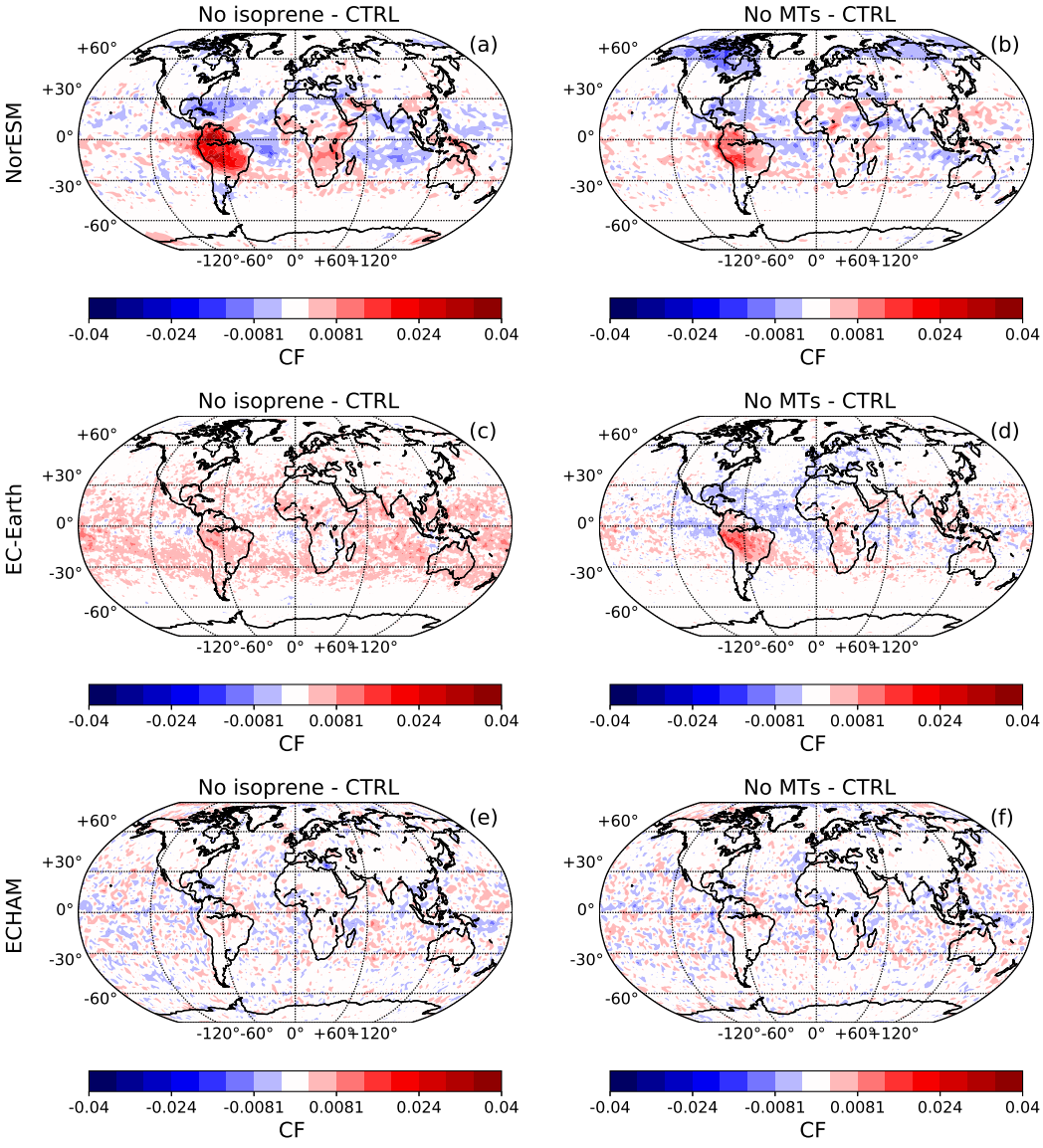

Figure S19. Maps of the difference in the average cloud fraction (CF) between the No isoprene (a, c and e) and No MTs (b, d and f) with respect to the CTRL simulation. This is shown for NorESM (a and b), EC-Earth (c and d) and ECHAM (e and f).

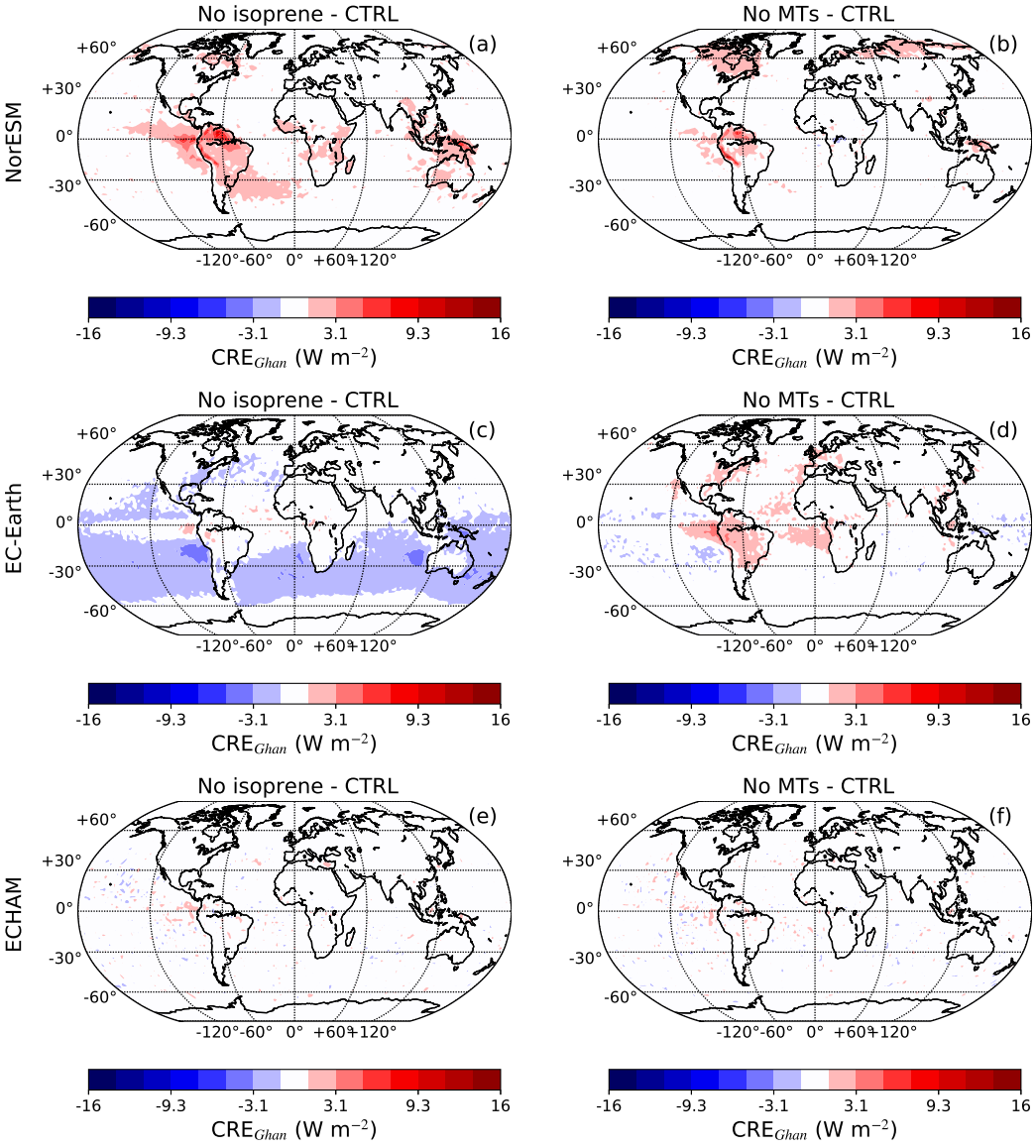

Figure S20. Maps of the difference in the average cloud radiative effect (CRE$_{Ghan}$) between the No isoprene (a, c and e) and No MTs (b, d and f) with respect to the CTRL simulation. This is shown for NorESM (a and b), EC-Earth (c and d) and ECHAM (e and f).

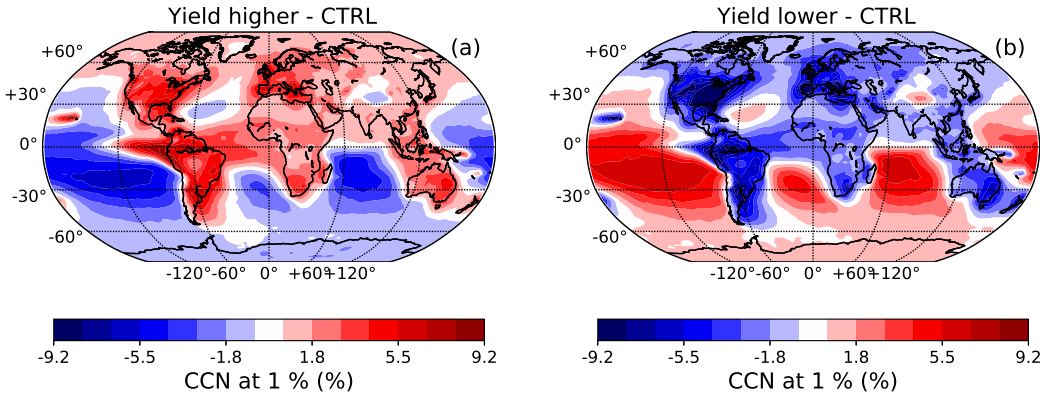

Figure S21. Maps of the difference in annually averaged cloud condensation nuclei at 1% supersaturation between the *Yield higher* and CTRL simulations (a) as well as the *Yield lower* and CTRL simulations (b) for EC-Earth. The CCN concentrations are averaged over for pressures over 850 hPa. The areas close to sources and remote are based on the changes in CCN concentrations in the Yield lower simulation (remote - positive and close to source - negative).